

# Mechanisms of Interphase Transport II: Theoretical Considerations and Experimental Evaluation of Interfacially Controlled Transport in Solubilized Systems

A. H. GOLDBERG\* and W. I. HIGUCHI

**Abstract** □ Equations were derived to describe the transport rate of a solute from an aqueous environment to an oil phase present as finely dispersed droplets. The basic diffusion equations included the effects of micellar solubilization in the aqueous phase and an interfacial barrier at the o/w interface. Two separate experimental systems were evaluated by fitting data to the rates predicted theoretically. System I was composed of polysorbate 80 as the surfactant, isopropyl myristate as the oil phase, and 2,3-bis-(*p*-methoxyphenyl)-indole as the drug solute. The second system was composed of mineral oil as the "sink," dibutyl phthalate as the solute, and polysorbate 80. The aqueous phase of System II contained 75% sucrose to increase the viscosity. The experimental transport rates of the solutes most closely fit the rates predicted by the theory which assumes that an interfacial barrier was rate determining.

**Keyphrases** □ Interphase transport, mechanisms—solubilized systems □ Interfacial barrier, effect—transport process □ Diffusion, effects—drug transport rates □ Oil phase, micron-sized spheres— infinite diffusion layer, production

In a previous report (1) mathematical relationships were presented that allowed predictions to be made for rates of transport of a solute from an aqueous solubilized system to a separate oil phase. The equations were based on first principles of diffusion, and considered two separate cases. The first case considered was that for simple diffusion, while the second case considered the diffusional aspects of an electrical barrier to the transport process. An experimental approach to the study of the rates of transport was outlined. This technique, based on the use of micron size oil droplets as the "sink," has a number of advantages over previously described methods.

This present report is concerned with another situation, that of an interfacial barrier, other than electrical, and its effect on the transport process. This report also presents the results of experimental studies with two different systems, embodying different solutes and different oil "sinks."

An experimental study of the role of adsorbed gelatin between the hexadecane-water interface has also been recently reported (2).

## THEORETICAL CONSIDERATIONS FOR INTERPHASE TRANSPORT INVOLVING A GENERAL INTERFACIAL BARRIER AND MICELLAR SOLUBILIZATION

In the case where the lipoidal phase consists of oil droplets, the barrier to the solute may arise from the interaction of the oil and the surfactant used to promote emulsification. The barrier may be in the form of monomeric adsorption of the surfactant onto the surface of the oil droplets.

The equations derived for transport through this barrier may be presented in a general form so as to provide a means of evaluating the magnitude of the barrier without foreknowledge of the existing molecular mechanism. This derivation is again based on the steady-state diffusion model for the transport of a solute into the spherical

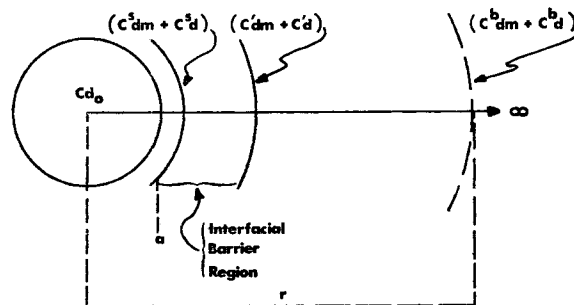


Figure 1—Illustration of diffusion of free drug plus drug in the micelles from the aqueous phase to an oil droplet "sink" in the presence of an interfacial barrier.

oil droplet. It assumes two rates,  $G_1$ , the rate through the aqueous phase, and  $G_2$ , the rate through the interfacial barrier of thickness  $l$ . The transport rate through the aqueous phase is denoted by

$$G_1 = 4\pi r^2(D_d dC_d/dr + D_{dm} dC_{dm}/dr) \quad (\text{Eq. 1})$$

This equation is integrated between the following limits (see Fig. 1):

$$\int_a^\infty dr/r^2 = 4\pi/G_1(D_d \int_{C_d'}^{C_d^b} dC_d + D_{dm} \int_{C_{dm}'}^{C_{dm}^b} dC_{dm}) \quad (\text{Eq. 2})$$

which leads to

$$G_1 = 4\pi(a + l)[D_d(C_d^b - C_d') + D_{dm}(C_{dm}^b - C_{dm}')] \quad (\text{Eq. 3})$$

The rate,  $G_2$ , through the interfacial barrier can be expressed as

$$G_2 = 4\pi r^2(P_{fd} dC_d/dr + P_{f_{dm}} dC_{dm}/dr) \quad (\text{Eq. 4})$$

where  $P_{fd}$ , the permeability coefficient of free drug through the interfacial film, may be defined as  $D_d k/l$ . The  $k$  suggests that this interfacial film is being treated as a separate phase. Likewise,  $P_{f_{dm}}$  may be defined as  $D_{dm} k'/l$ . If only one form of drug (e.g., the free drug) passes through the barrier, then the other form of drug (e.g., the micellized drug) has a permeability coefficient of zero. Assuming that the permeability coefficients are independent of oil droplet size and drug concentration, then integration of Eq. 4 from  $r = a$  to  $r = a + l$ ,  $C_d = C_d'$  to  $C_d = C_d^s$ , and  $C_{dm} = C_{dm}'$  to  $C_{dm} = C_{dm}^s$ , gives

$$G_2 = \frac{4\pi a(a + l)}{l} [P_{fd}(C_d' - C_d^s) + P_{f_{dm}}(C_{dm}' - C_{dm}^s)] \quad (\text{Eq. 5})$$

The utilization of the relationship (3)

$$C_{dm} = KC_d C_{saa} \quad (\text{Eq. 6})$$

and substitution into Eqs. 3 and 5 yields:

$$G_1 = 4\pi(a + l) \times \left[ \frac{D_d}{KC_{saa}} (C_{dm}^b - C_{dm}') + D_{dm} (C_{dm}^b - C_{dm}') \right] \quad (\text{Eq. 7})$$

or

$$G_1 = 4\pi(a + l) \left( \frac{D_d}{KC_{saa}} + D_{dm} \right) (C_{dm}^b - C_{dm}') \quad (\text{Eq. 8})$$

By the same mathematical manipulations Eq. 5 becomes

$$G_2 = \frac{4\pi a(a+l)}{l} \left( \frac{P_{fd}}{KC_{saa}} + P_{fdm} \right) (C_{dm}' - C_{dm}^s) \quad (\text{Eq. 9})$$

If Eq. 8 is solved for  $C_{dm}'$ , it is found that

$$C_{dm}' = C_{dm}^b - \frac{G_1}{(D_d/KC_{saa} + D_{dm})[4\pi(a+l)]} \quad (\text{Eq. 10})$$

Substituting this value for the  $C_{dm}'$  of Eq. 9 gives

$$G_2 = \frac{4\pi a(a+l)}{l} \left( \frac{P_{fd}}{KC_{saa}} + P_{fdm} \right) \times \left( C_{dm}^b - \frac{G_1}{[(D_d/KC_{saa}) + D_{dm}]4\pi(a+l)} - C_{dm}^s \right) \quad (\text{Eq. 11})$$

Under steady-state conditions,  $G_1 = G_2$ . Therefore, solving for  $G$  gives

$$G = \frac{[4\pi a(a+l)]l(P_{fd}/KC_{saa} + P_{fd})(C_{dm}^b - C_{dm}^s)}{1 + \{4\pi a(a+l)l(P_{fd}/KC_{saa} + P_{fdm})/[D_d/KC_{saa} + D_{dm}][4\pi(a+l)]\}} \quad (\text{Eq. 12})$$

Letting

$$D_e = \frac{D_d}{KC_{saa}} + D_{dm} \quad (\text{Eq. 13})$$

and

$$P_{fe} = \frac{P_{fd}}{KC_{saa}} + P_{fdm} \quad (\text{Eq. 14})$$

and substituting these into Eq. 12 yields

$$G = \left[ \frac{P_{fe}(a+l)}{D_e l + P_{fe} a} \right] 4\pi a D_e (C_{dm}^b - C_{dm}^s) \quad (\text{Eq. 15})$$

or

$$G = \Gamma 4\pi a \left( \frac{D_d}{KC_{saa}} + D_{dm} \right) (C_{dm}^b - C_{dm}^s) \quad (\text{Eq. 16})$$

If both the free and micelle-bound drug are capable of passing through the film, then  $\Gamma$  might be defined as

$$\Gamma = \frac{(P_{fd}/KC_{saa} + P_{fdm})(a+l)}{(D_d/KC_{saa} + D_{dm})l + (P_{fd}/KC_{saa} + P_{fdm})a} \quad (\text{Eq. 17})$$

If only one form of the drug is capable of film penetration,  $\Gamma$  might be defined as

$$\Gamma = \frac{(P_{fd}/KC_{saa})(a+l)}{(D_d/KC_{saa} + D_{dm})l + (P_{fd}/KC_{saa})a} \quad (\text{Eq. 18})$$

If the micelle disrupts upon entering the film, then it is possible to use Eq. 17 to define  $\Gamma$ , but the definition of  $P_{fdm}$  must be modified. In any event,  $\Gamma$  can be used to denote a general interfacial barrier constant.

After substituting the value of  $G$  from Eq. 16 into

$$G = V \frac{dC_{do}}{dt} \quad (\text{Eq. 19})$$

where  $V$  is volume (in milliliters of oil), the rate of uptake of solute by the oil can be expressed as

$$\frac{dC_{do}}{dt} = \frac{\Gamma 4\pi a}{V} \left( \frac{D_d}{KC_{saa}} + D_{dm} \right) (C_{dm}^b - C_{dm}^s) \quad (\text{Eq. 20})$$

When the concentrations of drug in the micelles ( $C^{dm}$  and  $C^s$ ) are transposed to oil concentration through the use of the apparent partition coefficient and a mass balance relationship, Eq. 20 can be written as (1)

$$\frac{dC_{do}}{dt} = \left( \frac{\Gamma 4\pi a}{V} \right) \left( \frac{D_d}{KC_{saa}} + D_{dm} \right) (\alpha - \beta C_{do}) \quad (\text{Eq. 21})$$

where

$$\alpha = \frac{T}{(1 + 1/KC_{saa})(1 - V)} \quad (\text{Eq. 22})$$

The  $T$  represents the total amount of solute per milliliter of emulsion. The second constant associated with this transformation is

$$\beta = V/(1 + 1/KC_{saa})(1 - V) + \left( \frac{1}{PC_{app}} - \frac{1}{PC_{olw}} \right) \quad (\text{Eq. 23})$$

This equation can be integrated to

$$C_{do} = \frac{\alpha}{\beta} \left\{ 1 - \exp. \left[ \frac{-\beta \Gamma A}{V} \left( \frac{D_d}{KC_{saa}} + D_{dm} \right) t \right] \right\} \quad (\text{Eq. 24})$$

where  $A = n4\pi a$ , with  $n$  representing the number of droplets, assuming a monodispersed system. This expression predicts that the change of concentration of drug in the oil exhibits the same dependency on time as does the aqueous diffusion model equation:

$$C_{do} = \frac{\alpha}{\beta} \left\{ 1 - \exp. \left[ \frac{-\beta A}{V} \left( \frac{D_d}{KC_{saa}} + D_{dm} \right) t \right] \right\} \quad (\text{Eq. 25})$$

(from Eq. 29, Reference 1), with the exception of the interfacial barrier constant,  $\Gamma$ , in the exponential term. As this constant,  $\Gamma$ , approaches unity, the model approaches the simple diffusion model; the greater the barrier to transport, the smaller the interfacial barrier constant.

Experiments may be designed to determine the presence or absence of a barrier to the transport of a drug from an aqueous to a lipid phase. If no barriers are present, all of the parameters involved could be independently determined, and theoretical values of  $C_{do}$  predicted. These predicted values could then be compared to the values for  $C_{do}$  obtained experimentally, and the curves matched. If the fit is poor, and it can be shown that there is no electrical barrier, then the experimental value of  $C_{do}$  and its respective time reduces Eq. 24 to one unknown which can then be solved for  $\Gamma$ . This value can then be used in Eq. 24 to predict  $C_{do}$  values for other experiments involving changes in the amount of oil used as the lipoidal sink, and in the initial drug concentrations. Values for  $\Gamma$  can also be obtained at several surfactant concentrations, and the dependence of the interfacial barrier upon surfactant concentration examined, at least qualitatively.

## EXPERIMENTAL

**General Considerations**—In order to find the operating mechanisms as proposed by the equations presented under *Theoretical Considerations*, experimental techniques must be used that would allow independent measurement of the involved parameters. These parameters may then be fitted to the equations, and theoretical values for the amount of drug in the oil can be calculated and then compared to those values experimentally determined.

There are many criteria to be considered in choosing the system for detailed study. The system is composed of three parts: the oil, the surfactant, and the drug. The oil phase chosen must have the ability to form emulsions that are stable over the time range of the transport experiments, and should present an uncharged surface to the aqueous phase. It is best if it is not solubilized to any great extent by the surfactant system chosen, since the volume and size of the oil droplets are assumed to remain constant. Also, solubilization of the oil by the surfactant could lead to dual transport rates occurring simultaneously; the oil being solubilized, and the solute entering the oil. The oil, in order to function as a sink, must be a good solvent for the drug being studied. Lastly the emulsion formed by the oil should produce uniform droplets of less than 10  $\mu$ .

The size and uniformity of the oil droplets are also a function of the surfactant and its concentration. The surfactant employed should not only be capable of producing this emulsion, but must be insoluble in the oil to prevent any dual transport or carrier effects. It must also serve to solubilize the drug. This solubilization should be a linear function of surfactant concentration for some reasonable range of surfactant. Linearity is necessary in order to evaluate the partition coefficient of the drug between the micellar and nonmicellar phases. For the initial studies, a surfactant which imparts no charge to either the oil or the micelle should be chosen.

As already mentioned in conjunction with the requirements for choosing an oil and a surfactant, the drug chosen must also

fit into these requirements. It must be capable of being solubilized by the surfactant; its partitioning between the micelle and the solvent must be constant; it must exhibit a high o/w partition coefficient; it must exhibit low water solubility, and it should be uncharged.

Experimentally, two cases will be examined, the aqueous diffusion controlled process and the interfacial barrier controlled process. These cases were investigated by the use of two separate systems. System I was composed of isopropyl myristate as the oil "sink," the nonionic surfactant polysorbate 80, and the nonionic drug, 2,3-bis-(paramethoxyphenyl)-indole.<sup>1</sup> Water was the solvent. After initial experimentation with this system, it was discovered that some isopropyl myristate was being solubilized by the polysorbate 80. Therefore, the aqueous phase of the system was changed from water to a saturated solution of isopropyl myristate in water or in water plus surfactant. All data collected independently of the rate experiments, as well as the rate experiments, were performed with the oil-saturated solvent. Additionally, further initial experimentation with System I showed that the rate of transport of a drug from the aqueous phase to the oil phase would be too rapid to measure physically, if the rate is controlled by diffusion through the aqueous phase. Assuming this might be true, and in order to facilitate physical measurements, a second system was chosen whose rate of diffusion through the aqueous phase would be much slower. System II was composed of mineral oil as the oil "sink," polysorbate 80 as the surfactant, and dibutyl phthalate as the drug. The solvent used consisted of water containing 75% sucrose. The sucrose was added to increase the viscosity approximately 20-fold. It was hoped that this viscosity increase would slow the rate of transport of an aqueous diffusion-controlled model enough for physical evaluation of the rates of transport. All data for this system, including the rate experiments, were collected using a 75% sucrose solution as the solvent.

**Analytical Procedures**—The only substances that required quantitative analyses were the drugs. The concentrations of both indoxole and dibutyl phthalate were determined spectrophotometrically.

Indoxole exhibits a  $\lambda_{\max}$  at 294  $\mu$  in 95% alcohol, with an absorptivity of 100.94  $\text{cm}^{-1} (\text{g/l.})^{-1}$ . The effect of various solvents, including solutions of polysorbate 80 do not significantly alter the absorptivity. Therefore, as long as the solvent was accounted for in the blank, the absorbance was found to be directly proportional to the concentration. The concentrations were calculated from the slope of the previously constructed Beer's law curve.

The concentrations of dibutyl phthalate were also determined spectrophotometrically at 274  $\mu$ , its wavelength of maximum absorbance. The absorptivity was found to be 4.474  $\text{cm}^{-1} (\text{g/l.})^{-1}$ . Similar to indoxole, the absorbance exhibited the same proportionality to the concentration, regardless of solvent, provided that the solvent used for dibutyl phthalate also appeared in the blank.

**Experimental Methods**—The testing of the equations previously outlined required that five different parameters be independently determined. These are, for both systems: 1. the solubility of the drug in both the solvent and the oil; 2. the diffusion coefficient of the drug in the solvents; 3. the equilibrium constant of partitioning of the drug between the micellar and nonmicellar phases; 4. the thermodynamic and apparent partition coefficients of the drugs between their respective oils and aqueous phases; 5. the particle size distribution of the emulsion; and 6. the rates of transport. Several assumptions, made under "Theoretical Considerations" must be shown to be valid. These are: that the particle size distribution does not change in the time it takes to complete a rate experiment, and that the micellar-nonmicellar partition coefficient exists, and is constant below saturation. Rate experiments can then be utilized to permit the evaluation of the theory.

**1. Solubility Studies**—An excess of indoxole, plus an excess of isopropyl myristate was added to distilled water, and shaken on a wrist action shaker<sup>2</sup> at 30.0° until equilibrium was attained. A portion of the suspension was rapidly filtered through a 100- $\mu$  pore size membrane.<sup>3</sup> The filtrate was suitably diluted and the indoxole concentration determined spectrophotometrically versus a similarly prepared blank.

The solubility of indoxole in isopropyl myristate was obtained in the same manner, *i.e.*, equilibration, filtration, dilution, and spectrophotometric analysis.

The solubility of dibutyl phthalate in the aqueous solvent was determined by adding an excess of the drug to 75% sucrose solution. The mixture was shaken at 30.0° on the wrist action shaker until equilibrium. A portion of the mixture was then filtered, and the concentration of dibutyl phthalate determined spectrophotometrically after suitable dilution.

Since dibutyl phthalate is totally miscible with mineral oil (the oil "sink"), no direct solubility of the drug in the oil could be obtained.

**2. Diffusion Coefficient Determinations**—The integral diffusion coefficients were determined from steady-state transport data through a membrane. The method used was reported previously (4), but was used with several modifications for determining  $D_{am}$ , the diffusion coefficient of the drug in the micelle. For a drug diffusing across a membrane, the rate can be defined at steady-state as

$$G = LD\Delta C \quad (\text{Eq. 26})$$

where  $G$  is the rate,  $D$  the diffusion coefficient,  $\Delta C$  the concentration gradient, and  $L$  the cell constant, derived experimentally from the diffusion of a drug for which the diffusion coefficient is known.

The solvent used for System II contained 75% sucrose. Therefore, it was necessary to determine if this great viscosity increase affected the cell constant. This was done by invoking the Stokes-Einstein relationship of the diffusion coefficient to the viscosity. This relationship shows the dependency

$$D = \frac{k}{\eta} \quad (\text{Eq. 27})$$

where  $\eta$  is the viscosity and  $k$  the other terms of the Stokes-Einstein equation. If this is valid, then

$$\frac{D_{\text{H}_2\text{O}}}{D_{\text{sucrose}}} = \frac{\eta_{\text{sucrose}}}{\eta_{\text{H}_2\text{O}}} \quad (\text{Eq. 28})$$

The ratio of the viscosities of benzoic acid solution, 0.01  $M$ , in 75% sucrose and in water was measured, and the theoretical diffusion coefficient of benzoic acid in 75% sucrose solution was calculated. A diffusion experiment of 0.01  $M$  benzoic acid in 75% sucrose solution was performed, and the cell constant,  $L$ , calculated, employing the theoretical diffusion coefficient previously calculated. The cell constants did not appear to be significantly different from the cell constants obtained from benzoic acid trials in water.

**3. Determination of the Micellar-Nonmicellar Partitioning Constant for the Solutes**—Previous reports have evaluated this constant using either the following relationship (3) or ones similar to it:

$$C_{dm} = KC_dC_{saa} \quad (\text{Eq. 6})$$

where  $K$  is the pseudo-equilibrium constant. The methods used to experimentally determine this constant have all been based on equilibrium data, and have assumed that this same  $K$  exists and is valid at concentrations below saturation. This is a reasonable assumption, and will be shown to be valid.

In order to determine  $K$  from saturation data, an excess of drug is added to solutions containing various concentrations of surfactant. At equilibrium, a graphing is made of the total amount of drug per volume in solution versus concentration of surfactant. Above the CMC, the slope of the linear portion of the curve equals  $K \cdot C_d$ , where  $K$  is the pseudo-equilibrium constant, and  $C_d$  is the concentration of drug solubilized by the solvent without surfactant present.

For System II, a different method had to be used to determine the approximate solubility of the drug in polysorbate 80 solutions, because the polysorbate 80 was soluble in the dibutyl phthalate. Ten culture tubes were filled with 10 ml. of solvent (75% sucrose in water plus surfactant). Dibutyl phthalate was added in increments of milligrams per milliliters of solvent, and allowed to equilibrate at 30.0°. At some point, no additional dibutyl phthalate was dissolved, and a cloudiness appeared. The concentration of dibutyl phthalate in the last clear tube was assumed to be the solubility of the dibutyl phthalate in that solvent. Six sets of these tubes were treated in a like manner, representing polysorbate 80 concentrations of 0.5 to 3.0%. The  $K$  obtained by this method is not the true ther-

<sup>1</sup> 2,3-Bis-(paramethoxyphenyl)-indole is the chemical name of the generic drug, indoxole, which was supplied by the Upjohn Co., Kalamazoo, Mich.

<sup>2</sup> Burrell Corp., Pittsburgh, Pa.

<sup>3</sup> Millipore Co., Bedford, Mass.

**Table I**—Solubilities of Indoxole and Dibutyl Phthalate

Drug	Solvent	Solubility, mg./ml.
Indoxole	Water saturated with iso-propyl myristate	$6.86 \times 10^{-4}$
	Isopropyl myristate	25.67
Dibutyl phthalate	75% Sucrose soln.	$2.57 \times 10^{-2}$
	Mineral oil	Total miscibility

modynamic value, but represents the minimum that the thermodynamic value would assume.

The value for  $K$ , below solute saturation concentration, can be shown to be constant and can be measured through the use of an intermediate immiscible phase. If the partitioning of a solubilized drug between an oil and a surfactant solution is examined, the expression for the apparent partition coefficient can be written as:

$$PC_{app.} = \frac{C_{do}}{C_{aq.}} = \frac{C_{do}}{C_d + C_{dm}} \quad (\text{Eq. 29})$$

where  $PC_{app.}$  is the apparent partition coefficient,  $C_{do}$  concentration of drug in the oil,  $C_{aq.}$  the concentration of drug in the aqueous phase (total surfactant solution concentration). The aqueous phase concentration then in turn can be expressed as the sum of the concentration found in the nonmicellar phase ( $C_d$ ) and the concentration of drug in the micellar phase ( $C_{dm}$ ). The reciprocal of Eq. 29 is

$$\frac{1}{PC_{app.}} = \frac{C_d}{C_{do}} + \frac{C_{dm}}{C_{do}} \quad (\text{Eq. 30})$$

If the value of  $C_{dm}$  is taken to be that expressed by Eq. 6 then Eq. 30 can be rewritten to

$$\frac{1}{PC_{app.}} = \frac{C_d}{C_{do}} + \frac{KC_d C_{saa}}{C_{do}} \quad (\text{Eq. 31})$$

The expression ( $C_d/C_{do}$ ) is actually the reciprocal of the true partition coefficient. When a graph is made of the reciprocal of the apparent partition coefficient versus the concentration of the surfactant, a straight line should result, with an intercept equal to the reciprocal of the thermodynamic partition coefficient and a slope equal to  $K \cdot C_d/C_{do}$ . If  $C_d$  is taken to be the saturation solubility of the drug in the solvent without surfactant present, and  $C_{do}$  is taken as the drug's oil solubility, the value for  $K$  can be calculated. This value can be obtained at any degree of saturation of the aqueous phase.

**4. Determination of the Apparent Partition Coefficient**—Several methods exist for determining the partition coefficient of a drug between an oil phase and an aqueous phase. The following method was chosen. A known volume of oil was added to a known volume of aqueous phase containing predetermined concentrations of drug and surfactant. This two-phase system was then shaken on a shaker at 30.0° until the drug was equilibrated between the two phases.

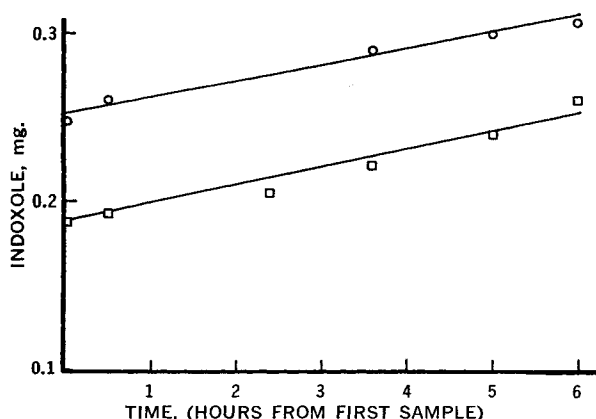


**Figure 2**—Diffusion rate data of indoxole in 1.0% polysorbate 80 through the diffusion cell.

The aqueous phase was then separated from the oil phase by filtration and the drug concentration within the aqueous phase determined. The amount of drug initially present, minus the amount of drug found in the aqueous phase at equilibrium, represents the amount of drug in the oil. This amount divided by the volume of oil equals the concentration of drug in the oil at equilibrium. The equilibrium concentration of drug in the oil (mg./ml.) divided by the equilibrium concentration of drug in the aqueous phase (mg./ml.) is the apparent o/w partition coefficient.

The thermodynamic partition coefficient is defined as the partitioning of the drug between the oil and the pure solvent. For System I, the thermodynamic partition coefficient of indoxole between isopropyl myristate and water saturated with isopropyl myristate, could not be obtained experimentally due to the extremely low water solubility and high oil solubility of indoxole. Therefore, this value was assumed to be the solubility (mg./ml.) of indoxole in isopropyl myristate divided by the solubility (mg./ml.) of indoxole in water saturated with isopropyl myristate. For a similar reason, the high oil and low aqueous solubility of dibutyl phthalate, the thermodynamic partition coefficient for System II also could not be experimentally determined. In addition, since the dibutyl phthalate is completely miscible with the mineral oil, no oil solubility could be determined. Therefore the reciprocal of the intercept obtained from a graphing of  $1/PC_{app.}$  versus  $C_{saa}$  was assumed to be the true partition coefficient.

**5. Particle Size Distribution Determination**—The particle size determinations and the distribution of particle sizes was determined using a counter<sup>4</sup> and a particle analyzer.<sup>5</sup> Mass balance was evaluated by determining the phase volume of oil present in a given volume of sample. The phase volume ( $\phi$ ) of the particles can be expressed as

$$\phi = \int n(V) V dV \quad (\text{Eq. 32})$$

where  $n(V)$  is the number of particles of volume  $V$ . A graph is made of  $n \cdot V$  versus  $V$ . The area under such a curve represents the total volume of particles present, per total volume of sample tested.

In the systems employed in this study, the particles are formed by emulsification of the oil used as the sink. The particle size distribution of the emulsion droplets was checked initially, as well as after the rate experiments to ensure that the particle size distribution did not change. A value for the radius of the particles to be used in the theoretical calculations can be determined from the particle size distribution. If it is assumed that the emulsion is composed of uniformly sized droplets of that radius, then by

$$n \cdot \frac{4}{3}\pi r^3 = \text{total volume of oil present} \quad (\text{Eq. 33})$$

a value for the number of particles present can be calculated.

**6. Rate Experiments**—In order to perform rate experiments with the emulsion systems, a technique was developed that allowed rapid separation of the oil phase from the aqueous phase (5). To perform the rate determinations, stock solutions were prepared varying in both surfactant concentration and drug concentration. An emulsion stock was also prepared. At time zero, an amount of the emulsion was added to the stock solution of drug and surfactant in proportion to the oil concentration desired. The flask was then shaken at 30.0°. Samples of at least 3 ml. were withdrawn at appropriate time intervals and immediately filtered. When approximately one-half of the sample was filtered, the time was recorded and taken to be the time at which the sample was taken. Each sample was then suitably diluted, and analyzed for the drug concentration. The amount of drug that had been lost from the aqueous phase was assumed to be in the oil phase. That amount of drug, divided by the amount of oil present, was denoted as the concentration (mg./ml.) of drug in the oil ( $C_{do}$ ) at that time.

In System I, the stock emulsion of 10% isopropyl myristate was prepared by adding 3 ml. of isopropyl myristate to 27 ml. of a 1% polysorbate 80 solution, previously saturated with isopropyl myristate, in a 100-ml. shaking cylinder. After shaking, the emulsion was passed three times through a hand homogenizer. The emulsion was then placed on a wrist action shaker to permit the completion of the rapid phase of coalescence.

<sup>4</sup> Coulter Electronics, Franklin Park, Ill.

<sup>5</sup> 400 Channel R.I.D.L., Radiation Instrument Development Laboratories, Melrose Park, Ill.

**Table II**—Data from Diffusion Coefficient Studies

Drug	Solvent	Cell Constant	Concn. Employed, mg./ml.	G-, mg./sec. × 10 <sup>6</sup>	D <sub>e</sub> <sup>a</sup> , cm. <sup>2</sup> sec. <sup>-1</sup>	D <sup>b</sup> , cm. <sup>2</sup> sec. <sup>-1</sup>
2,3-Bis-(para-methoxyphenyl)-indole	1% Polysorbate 80 saturated with IPM <sup>c</sup>	17.07	0.2408	2.889	7.03 × 10 <sup>-7</sup>	—
		17.28	0.2408	3.500	8.41 × 10 <sup>-7</sup>	—
	H <sub>2</sub> O saturated with IPM <sup>c</sup>	—	—	—	Mean 7.72 × 10 <sup>-7</sup>	Mean 7.62 × 10 <sup>-7b</sup> 6.38 × 10 <sup>-8d</sup>
Dibutyl phthalate	0.5% Polysorbate 80 in 75% sucrose soln.	84.49	0.5454	1.485	3.22 × 10 <sup>-8</sup>	—
		88.03	0.5454	1.916	3.99 × 10 <sup>-8</sup>	—
	1.0% Polysorbate 80 in 75% sucrose soln.	84.11	1.1120	3.044	Mean 3.61 × 10 <sup>-8</sup>	Mean 3.13 × 10 <sup>-8b</sup>
		96.39	1.1120	3.488	3.26 × 10 <sup>-8</sup>	—
					3.25 × 10 <sup>-8</sup>	—
	2.0% Polysorbate 80 in 75% sucrose soln.	97.28	2.1234	3.86	Mean 3.26 × 10 <sup>-8</sup>	Mean 3.01 × 10 <sup>-8b</sup>
		102.33	2.1234	4.08	1.87 × 10 <sup>-8</sup>	—
					1.88 × 10 <sup>-8</sup>	—
	75% Sucrose	—	—	—	Mean 1.87 × 10 <sup>-8</sup>	Mean 1.74 × 10 <sup>-8b</sup> 2.30 × 10 <sup>-7e</sup>

<sup>a</sup> Calculated from Eq. 26. <sup>b</sup> Calculated from Eq. 34. <sup>c</sup> IPM = isopropyl myristate. <sup>d</sup> Calculated from Eq. 35. <sup>e</sup> Calculated from Eqs. 35 and 28.

For the rate determinations, 20 ml. of drug-polysorbate 80 stock solution was placed into a 50-ml. volumetric flask. At time zero, 5 ml. of the emulsion was added to this flask. Samples were withdrawn at suitable time intervals and immediately filtered. After suitable dilution of each sample, the indoxole concentration was determined by spectrophotometric analysis.

For System II, the stock emulsion was prepared by adding 150 ml. of aqueous phase, consisting of 75% sucrose and 0.1% polysorbate 80, to a blender.<sup>6</sup> The blender was started and 50 ml. of mineral oil was added very slowly. At the end of 5 min., the blender was turned off, and the emulsion placed on a wrist action shaker (Burrell) for 24 hr. to permit the completion of the rapid phase of coalescence.

For the rate experiments, either 4 ml. of emulsion was added to 46 ml. of drug stock solution (2% final oil concentration) or 2 ml. was added to 48 ml. of stock solution (1% final oil concentration). The concentration of drug in the stock solution varied with the experiment.

**RESULTS AND DISCUSSION**

The results of the experiments of each system will be detailed separately. The significance of each result will be discussed sequentially, but the overall relationships will be presented when the results of the rate experiments are discussed.

**1. Solubility Studies**—The solubilities of indoxole in the solvent (distilled water saturated with isopropyl myristate) and in the oil (isopropyl myristate) are shown in Table I. The solubilities of dibutyl phthalate in its solvent (75% sucrose solution) and its oil phase (mineral oil) is also given in Table I.

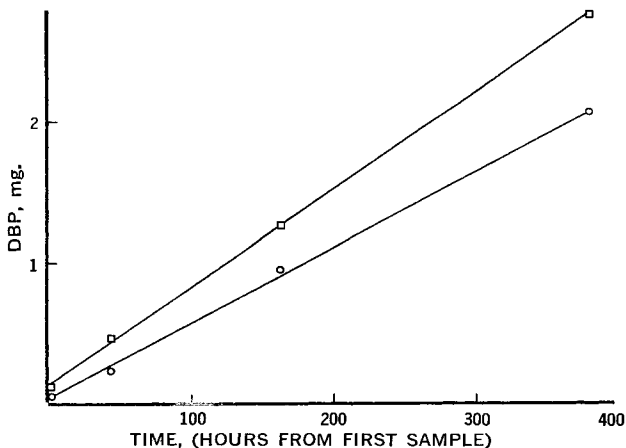


**Figure 3**—Diffusion rate of dibutyl phthalate in 75% sucrose solution containing 0.5% polysorbate 80 through the diffusion cell.

**2. Diffusion Coefficient Determinations**—The water solubility of indoxole is so low as to make experimental determination of its diffusion coefficient in water unfeasible. However, the value of D<sub>a</sub> was computed using the Stokes-Einstein equation

$$D = \frac{kT}{6\pi\eta r} \tag{Eq. 34}$$

where *k* is the Boltzman constant, *T* the absolute temperature, *η* the density of the solvent, and *r* the radius of a single molecule. The value of D<sub>a</sub>, the diffusion coefficient of indoxole in the solvent, calculated in this manner is 4.38 × 10<sup>-6</sup> cm.<sup>2</sup> sec.<sup>-1</sup>.

The diffusion coefficient of indoxole in 1.0% polysorbate 80 solution presaturated with isopropyl myristate was determined using the cells previously described (4). A filter,<sup>7</sup> 37 mm. and 0.9 μ pore size, was used as the membrane. The rate of transport of indoxole from Flask II to Flask I of the diffusion cell is shown in Fig. 2. The cell constants, concentration, etc., are tabulated in Table II. The diffusion coefficient, as derived by using the rate of transport data in Eq. 26, is really the effective diffusion coefficient. The integral diffusion coefficient of the drug in the micelle, D<sub>dm</sub>, is calculated from the following relationship

$$D_e = \frac{D_d C_d + D_{dm} C_{dm}}{C_d + C_{dm}} \tag{Eq. 35}$$

For indoxole in 1% polysorbate 80 presaturated with isopropyl myristate, D<sub>e</sub> is found to be 7.72 × 10<sup>-7</sup> cm.<sup>2</sup> sec.<sup>-1</sup>, and D<sub>dm</sub> calculated to be 7.62 × 10<sup>-7</sup> cm.<sup>2</sup> sec.<sup>-1</sup>.

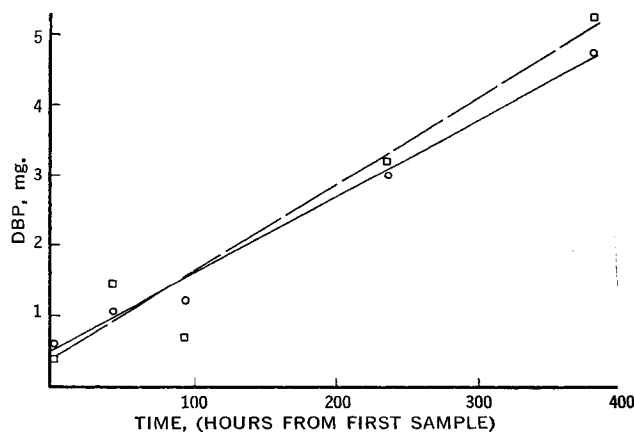


**Figure 4**—Diffusion rate of dibutyl phthalate in 75% sucrose solution containing 1.0% polysorbate 80 through the diffusion cell.

<sup>6</sup> Waring Products Division, Winsted, Conn.  
<sup>7</sup> Gelman Industries, Ann Arbor, Mich.

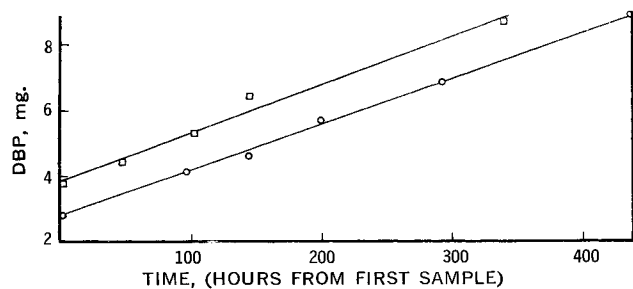


Figure 5—Diffusion rate of dibutyl phthalate in 75% sucrose solution containing 2.0% polysorbate 80 through the diffusion cell.

The water solubility of dibutyl phthalate was also too low for experimental determination of its diffusion coefficient; therefore, it was calculated by means of Eq. 34. The theoretical value was found to be  $4.70 \times 10^{-6}$  cm.<sup>2</sup> sec.<sup>-1</sup> in water. However, the solvent employed in this second system is 75% sucrose solution. By measuring the relative viscosity of a 75% sucrose solution (20.46) and using Eq. 28, the diffusion coefficient of dibutyl phthalate in 75% sucrose solution is calculated to be  $2.30 \times 10^{-7}$  cm.<sup>2</sup> sec.<sup>-1</sup>.

The diffusion coefficients of dibutyl phthalate in solutions varying in surfactant concentrations were experimentally determined in the previously described cells using a silver membrane.<sup>8</sup> The effective diffusion coefficients were calculated using Eq. 26 and rates of transport data shown in Figs. 3-5. The integral diffusion coefficients, calculated using Eq. 35, are reported in Table II along with the other parameters involved in their determination.

Before determining the diffusion coefficients, it had been discovered that the sucrose solutions promoted mold growth upon standing. Therefore, since about 3 weeks were required for the determination of the diffusion coefficients, all solutions had to be sterilized before use. The sucrose was sterilized by ethylene oxide gas and the polysorbate 80 solutions of various concentrations by passing the solutions through a silver filter of 0.2  $\mu$  pore size. Under aseptic conditions the preweighed sucrose was quantitatively transferred to presterilized volumetric flasks, the polysorbate 80 solutions added, and brought to volume with sterile water for injection, USP. The cells were sterilized with alcohol, and filled aseptically. Sampling was performed, as aseptically as possible, using sterile pipets.

**3. Determination of the Micellar-Nonmicellar Equilibrium Constants**—As discussed under *Experimental Methods*, this constant is derived from the slope of the line obtained from equilibrium solubility studies above the CMC of the surfactant. The results obtained for the indoxole-polysorbate 80 system are graphically shown in Fig. 6. The slope of this line (determined by least squares) was found to be 0.532. When this value is divided by  $C_d$  ( $6.86 \times 10^{-4}$  mg./ml.) it yields the value 775.51. This is the pseudo-equilibrium constant for the partitioning of indoxole between the micellar and nonmicellar phases.

The results for the dibutyl phthalate system are depicted in

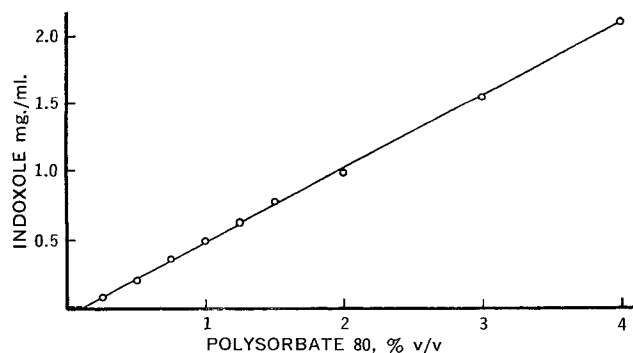


Figure 6—Equilibrium solubilities of indoxole as a function of polysorbate 80 concentrations.

<sup>8</sup> Selas Flotronics, Spring House, Pa. Flotronics membrane 37 mm., 1.2  $\mu$  pore size.

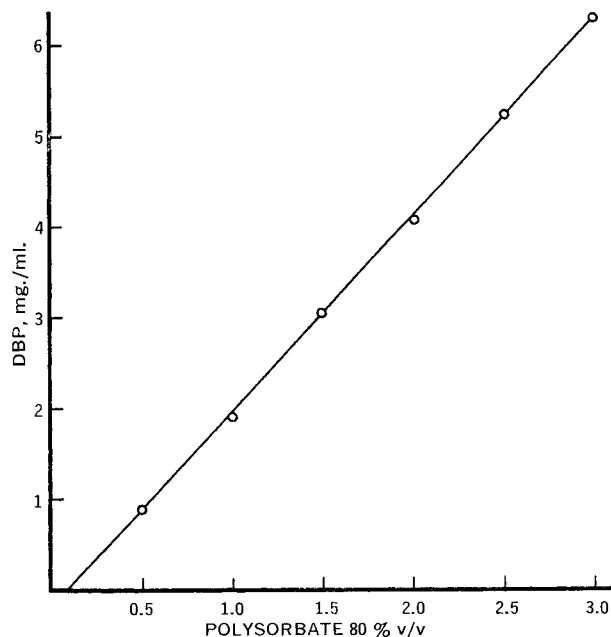


Figure 7—Equilibrium solubilities of dibutyl phthalate as a function of polysorbate 80 concentrations.

Fig. 7. The slope of this line (determined by least squares) was found to be 2.178. When this value is divided by the solubility of dibutyl phthalate in 75% sucrose without surfactant present ( $2.57 \times 10^{-2}$  mg./ml.), it yields the pseudo-equilibrium constant of 84.73. The linearity of the data from both systems indicates that above the CMC, the additional surfactant increases the number of micelles, but does not alter the size and/or shape of the micelles at the surfactant concentrations employed.

Evidence for the constancy of these  $K$  values below solute saturation concentrations is presented under the subheading of *Determination of the Apparent Partition Coefficient*.

**4. Determination of the Apparent Partition Coefficient**—Table III lists the partition coefficients, the volumes of aqueous phase, and the initial concentrations used to study the apparent partition coefficients of indoxole between isopropyl myristate and various concentrations of polysorbate 80. Figure 8 shows the relationship between the reciprocal of the partition coefficient to the concentration of surfactant employed. The solid line is theoretical, being derived from solubility data obtained at saturation. The points were experimentally determined from partition coefficient data at concentrations below saturation. The fact that the two slopes (the theoretical and the experimental) are in agreement indicates the validity of the assumption that there exists a  $K$  between  $C_{dm}$  and  $C_d$  that holds below as well as at saturation. The line appears to pass through the origin, however, it has an extremely small intercept due to the high thermodynamic o/w partition coefficient. This partition coefficient is chosen as  $C_{do}/C_{aq}$  and is calculated to be  $3.74 \times 10^4$ .

Similarly, the results of the partitioning experiments of dibutyl phthalate between mineral oil and 75% sucrose solutions containing various concentrations of surfactant is given in Table III and Fig. 9. Table IV gives the results of a study that shows the constancy of the partition coefficients as functions of both drug and oil concentrations. The reciprocal of the intercept of the line in Fig. 9 denotes the o/w partition coefficient of dibutyl phthalate, and was found to be 667.0. This value represents the minimum value, as previously discussed under *Experimental Methods*.

**5. Particle Size Distribution Determination**—The particle sizes of the droplets formed when isopropyl myristate was emulsified with polysorbate 80 were measured with the counter using a 30- $\mu$  aperture tube and with the particle analyzer using calibrations of 1.17  $\mu$  diameter latex particles. The mass balance calculated using this data and Eq. 32 was approximately 20% of the oil added; thus indicating that 80% of the oil was present as droplets with radii smaller than 0.585  $\mu$ . The largest particles found had radii of 1.13  $\mu$ , but were very few in number (see the 160th channel in Fig. 10). This size range was verified by microscopic examination. For calculations involving the radii of the particles, it was assumed

**Table III—Apparent Partition Coefficients for Indoxole and Dibutyl Phthalate**

Polysorbate 80, %	Initial Drug Concn., mg./ml.	Saturation, %	Vol. of Aqueous Phase, ml.	Vol. of Oil Phase, ml.	Partition Coefficient
<b>2,3-Bis-(paramethoxyphenyl)-indole</b>					
0.25	0.0510	56.9	20	0.5	220.72
0.50	0.1174	52.7	20	0.5	81.66
0.75	0.1744	49.0	20	1.0	66.55
1.00	0.2849	58.3	20	1.0	48.81
1.25	0.3022	48.6	20	1.0	34.26
1.50	0.3607	47.8	20	1.0	33.48
1.75	0.4281	48.2	20	1.0	27.94
2.00	0.5252	51.4	20	1.0	23.62
<b>Dibutyl phthalate</b>					
0.5	0.2408-0.6021	—	50	(0.1-0.2)	127.15
1.0	0.4816-1.2042	—	50	(0.5-1.0)	60.13
1.5	1.0838-1.8062	—	50	(1.0-2.0)	44.90
2.0	1.4450-2.4082	—	50	(1.0-2.0)	33.41

that the majority of particles had radii of 0.5  $\mu$ . Assuming monodispersity, the number of particles present was calculated using Eq. 33 and was found to be  $3.9 \times 10^{10}$  particles per milliliters of emulsion containing 2.0% isopropyl myristate.

A different emulsion was employed for the dibutyl phthalate-mineral oil system, whose particle size was much coarser. The data are shown in Fig. 11. A 50- $\mu$  aperture tube was used, and was calibrated with latex particles having a diameter of 2.05  $\mu$ . The singlet peak appears on the 20th channel, the doublet on the 50th channel, and the triplet on the 80th channel (see Fig. 11). The mass balance found from the data (Fig. 12) and Eq. 33 was about 67% of the oil added. Therefore, only 33% of the oil present had a particle size of less than 1.025  $\mu$  radius. By dividing the area under the curve (see Fig. 12) in half, it was determined that the middle third of the volume of oil was composed of oil droplets having radii between 1.025 and 1.215  $\mu$ . The mean of these values, 1.12  $\mu$ , was used for calculations requiring the radius of the oil droplet. Assuming monodispersity and using this value in Eq. 33 gives the number of droplets present as  $2.52 \times 10^9$  per milliliter of emulsion for a 2% mineral oil emulsion.

The ability to reproduce the particle size distribution from one emulsion to another is shown in Figs. 13a and 13b. The emulsion in Fig. 13a was prepared separately from the emulsion shown in Fig. 13b. It was also assumed under *Theoretical Considerations* that the particle size distribution remains constant for the duration of the rate experiments. A comparison of the size distributions obtained at the start of a rate determination, and 2 hr. after the experiment, validates this assumption (see Fig. 13c).

**6. Rate Experiments**—The results of the rate experiments will be discussed in relation to the three mechanisms proposed, *i.e.*, the simple diffusion model, the interfacial barrier model, and the electrical barrier model. Also, under each of these divisions, the indoxole-isopropyl myristate-polysorbate 80 system will be discussed separately from the dibutyl phthalate-mineral oil-polysorbate 80 system.

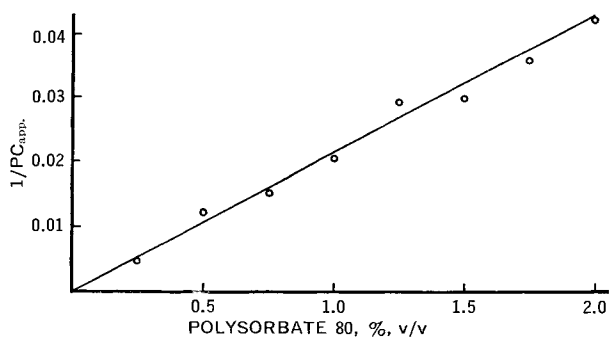


**Figure 8—Reciprocal of the apparent partition coefficients of indoxole as a function of polysorbate 80 concentration. Key: Solid line, theoretical line from solubility data; points, experimentally determined data.**

**CASE A—Simple Diffusion**—The first studies involved the indoxole-isopropyl myristate-polysorbate 80 system. Initial rate experiments presented the first obstacle, dual transport. This is depicted in Fig. 14, which shows the rate of loss of indoxole from a 1% polysorbate 80 solution to the isopropyl myristate oil droplets. The first sample time (10 min.) has the lowest concentration found in the aqueous phase. The next several points indicate that the indoxole is returning to the aqueous phase, until approximately 180 min. have elapsed, when an equilibrium is established. If partition coefficient data is used to predict the equilibrium value, the predicted value is 48% lower than the equilibrium actually established. When the portion of the curve depicting the reappearance of the indoxole in the aqueous phase is extrapolated to time zero, the intercept for the concentration of indoxole is exactly that concentration predicted for the equilibrium value from partition coefficient data. From this data it was hypothesized that the isopropyl myristate was being dissolved by the polysorbate 80 aqueous phase, thereby changing the apparent partition coefficient. When this experiment was repeated using an aqueous phase presaturated with isopropyl myristate, indoxole did not reappear in the aqueous phase. Therefore, it was decided that all aqueous solutions should be presaturated with isopropyl myristate and used for data collected for this system.

New rate experiments were performed using oil presaturated solvents (polysorbate 80, 1 and 2%) and sampled at approximate 60-sec. intervals. Measurable amounts of indoxole were transported into the lipid phase, as depicted in Fig. 15. When the separately measured parameters were fitted to Eq. 25 and values for  $C_{ao}$  (the concentration of indoxole in the isopropyl myristate) were calculated, it was seen that the experimental rate of transport was ex-

**Table IV—Data from Dibutyl Phthalate Partition Coefficient Studies**

Polysorbate 80, %	DBP <sup>a</sup> /mg. 50 ml.	Mineral Oil, ml.	Partition Coefficient, apparent
0.5	12.04	0.1	129.36
	30.10	0.2	124.95
		Mean	127.15
1.0	24.08	0.5	58.22
	36.12	1.0	62.59
	60.21	1.0	59.59
		Mean	60.13
1.5	54.19	1.0	46.43
	72.25	1.0	44.13
	90.31	1.0	48.07
	90.31	2.0	40.98
		Mean	44.90
2.0	72.25	1.0	31.63
	120.41	1.0	35.38
	120.41	2.0	33.23
		Mean	33.41

<sup>a</sup> Dibutyl phthalate.

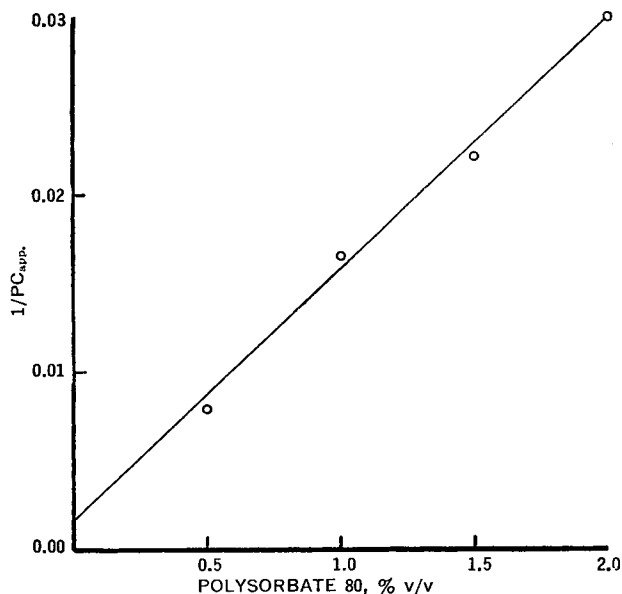


**Figure 9**—Reciprocal of the apparent partition coefficients of di-butyl phthalate as a function of polysorbate 80 concentration.

ceedingly slow as compared to the theoretical simple diffusion rates (see Fig. 15). In fact, theoretically, equilibration should have occurred in less than 1 sec. The insight gained from these experiments was that Eq. 25 was valid for predicting equilibrium values, thus indicating that the limits of integration used in deriving the equation

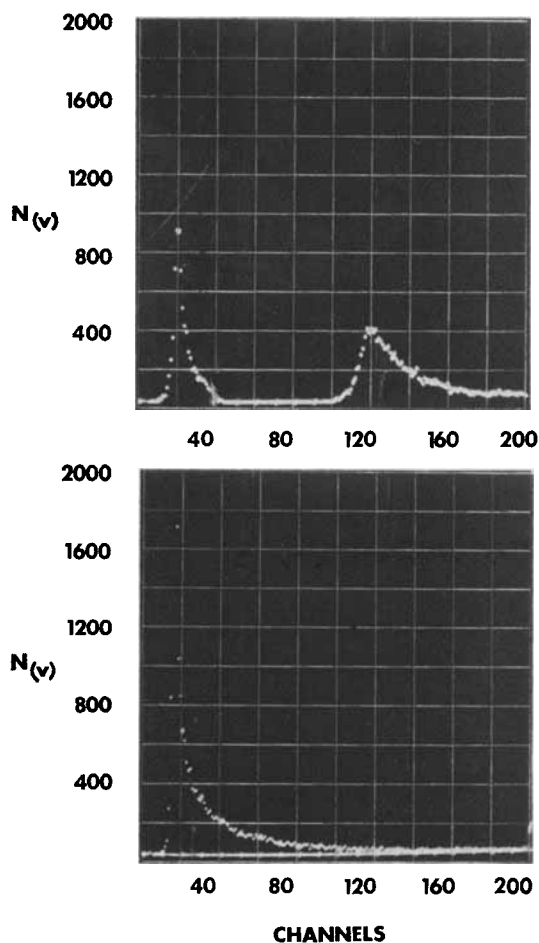


**Figure 10**—Particle size distribution of the isopropyl myristate emulsion.

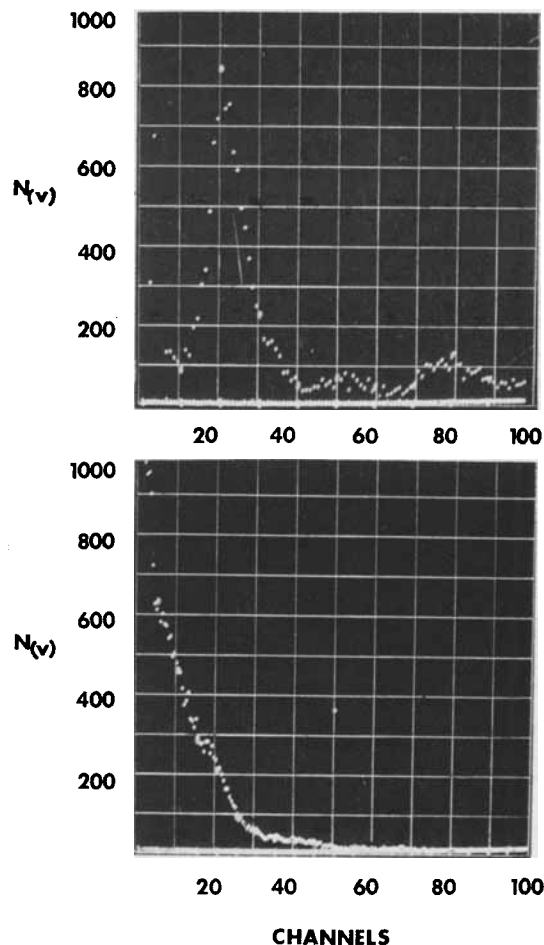


**Figure 11**—Particle size distribution of the mineral oil emulsion.

was correct. However, examination of the results of these experiments with Eq. 25 also indicated that diffusion through the aqueous phase was not rate limiting. It was then postulated that there might be an interfacial barrier present, that would reduce the rate, and would give  $\Gamma$ , the interfacial barrier constant a value less than one. One of the possible barriers conceived of was steric arrangement of the polar portion of the isopropyl myristate molecule. Another was an interaction at the surface of the oil droplet between the isopropyl myristate and the polysorbate 80.

To minimize the possible effects of a polar oil, isopropyl myristate was changed to mineral oil. Unfortunately, indoxole was not sufficiently soluble in the mineral oil, thereby necessitating selection of a

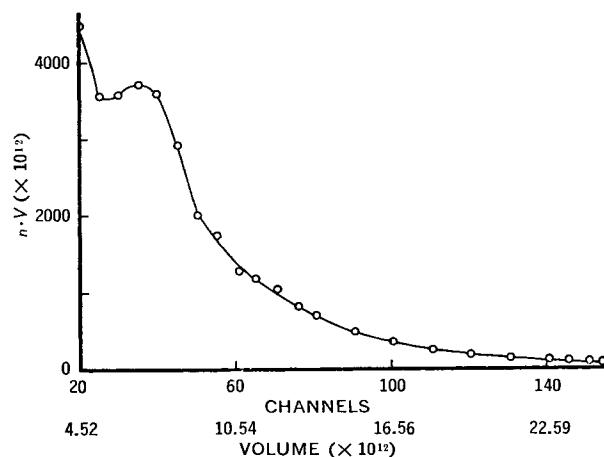


**Figure 12**—Integral curve used to find the phase volume of the mineral oil emulsion.



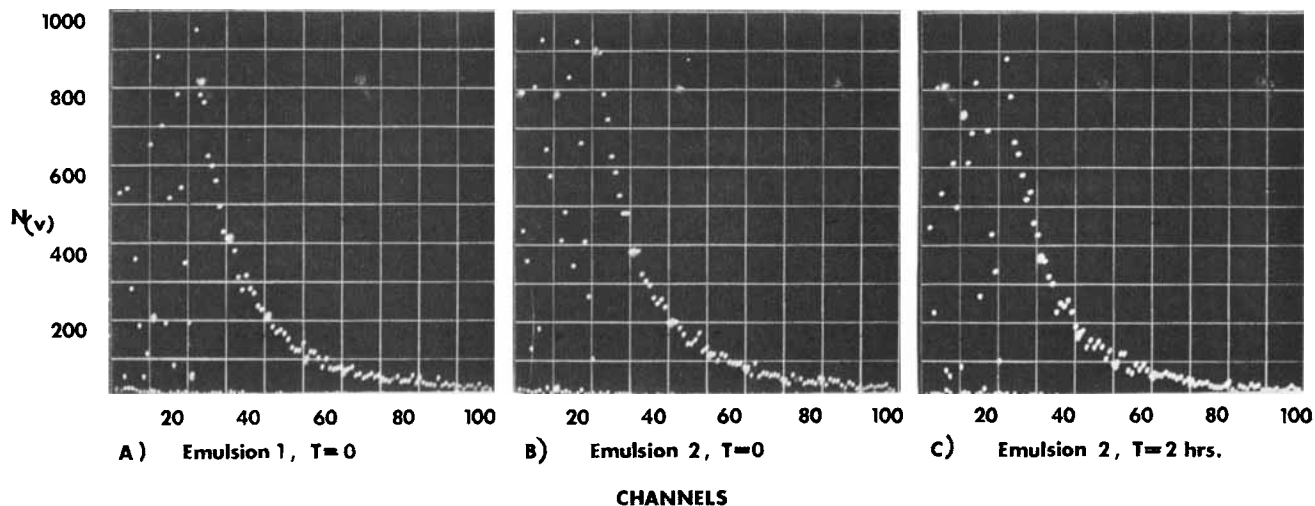


Figure 13—Comparison of the particle size distributions of a mineral oil emulsion as a function of reproducibility and time.

new drug which satisfied the requirements listed in the *General Considerations* section of *Experimental*. Dibutyl phthalate was selected as the drug, and the surfactant polysorbate 80 was used again in this study. It was also decided to increase the viscosity of the aqueous phase to possibly slow the rate to facilitate physically measuring the amounts of dibutyl phthalate transported. All parameters such as partition coefficients, solubilities, diffusion coefficients, etc., were determined using 75% sucrose as part of the solvent. All emulsions were also prepared containing 75% sucrose in the aqueous phase. By trial and error it was discovered that emulsions prepared with 25% mineral oil in 2.0% polysorbate 80 and 75% sucrose in the aqueous phase produced rates of transport too rapid to measure. However, when the percentage of polysorbate 80 in the aqueous phase was reduced to 0.1%, rates of transport were achieved that were easily measured. This emulsion formulation was then used in all further rate determinations.

All the rate experiments were performed using the wrist action shaker to maintain homogeneity throughout the system. The speed control handle was set at the 1.5 position. If the chosen setting was increased to 3.5, the contents splashed slightly over the top of the container. However, when the results of a rate experiment performed at the 3.5 setting is compared to the results obtained at the 1.5 setting (Fig. 16) it is observed that there is only a small change in rates of transport as a result of a large change in shaking rate.

Rate experiments involving various concentrations of surfactant, drug and oil were conducted, and the results are shown in Figs. 17-21. The solid lines represent a visual fit of the data points. Figure 17 represents the rates of transport of dibutyl phthalate from the aqueous phase to the mineral oil which comprises 2% of the total volume of the system. The concentrations of dibutyl phthalate employed are in the relative concentrations of 1, 2, and 4, while the surfactant concentrations are about 0.5, 1.0, and 2.0%, respectively. This combination of relative concentration and surfactant concentration was used to keep the percent saturation of the aqueous phase constant. The 2.0% surfactant solution, which

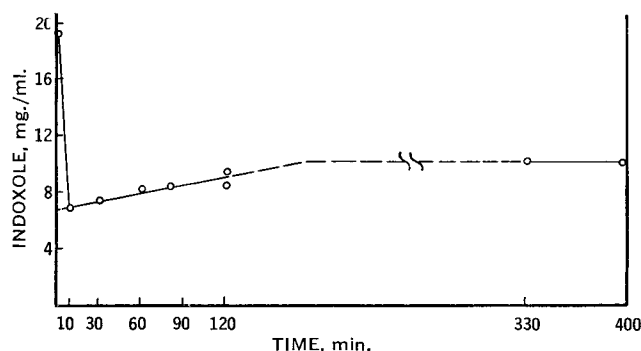


Figure 14—Preliminary study of the rate transport of indoxole from 1.0% polysorbate 80 solution to the isopropyl myristate.

contains the greatest amount of drug, produces the greatest concentration of drug in the oil. The equilibrium values obtained from the rate data fit the equilibrium values predicted from data collected independently quite well. However, when the independent data are used to solve for theoretical  $C_{a0}$  values based on simple diffusion (Eq. 25), there is no agreement, as can be seen by comparing the theoretical values (represented by the dashed line, Figs. 17-21) and the experimental data.

Rate data obtained when the concentration of drug is maintained constant, while the concentration of surfactant varies, are shown in Fig. 18. Equilibrium values again agree with theory. The system providing the highest values for the dibutyl phthalate concentration in the mineral oil is the 0.5% surfactant. This equilibrium is governed by the apparent partition coefficient. Again the equation, designed for simple diffusion (Eq. 25), fails to predict the proper time dependency for the rate of transport.

Figures 19-21 show the transport data for dibutyl phthalate from the aqueous phase to the mineral oil. At each concentration of surfactant, the drug concentrations were about the same, but the volume of mineral oil was changed from 2 to 1% of the system's volume. Once again the simple diffusion equation was valid for equilibrium conditions, but not for the time dependency of the transport process.

From these results, it is evident that the simple diffusion equation did not suitably predict the concentration of drug in the oil as a function of time, despite the agreement with equilibrium data. Since the rate of transport of a drug from a solubilized system to an oil phase in the form of small spheres is not controlled by diffusion

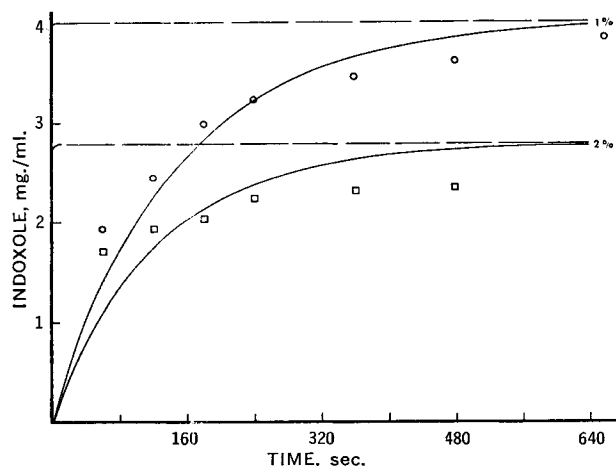
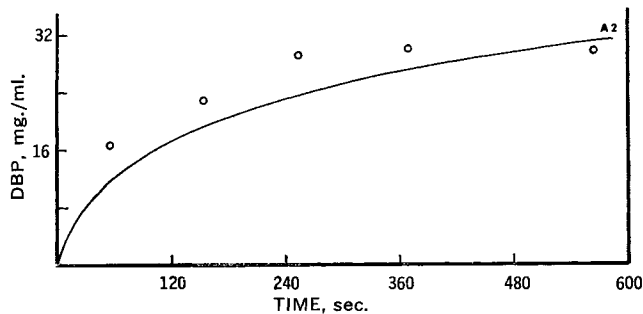


Figure 15—The appearance of indoxole in the oil as a function of time. Key: points, experimental data; dashed line, the theoretical rate of transport based on diffusion theory; solid line, the theoretical rate based on the interfacial barrier theory.



**Figure 16**—The appearance of dibutyl phthalate in the oil as a function of time and shaking rate. The circles represent the rapid speed, the solid line the normal speed of shaking.

through the aqueous phase, another rate determining process must be considered.

**Case B—Interfacial Barrier**—In the *Theoretical Considerations* section, this “film” is accounted for in the transport rate equation by assuming that the solute(s) have some permeability coefficient(s) for passage through the film. The final equation (Eq. 24) is very

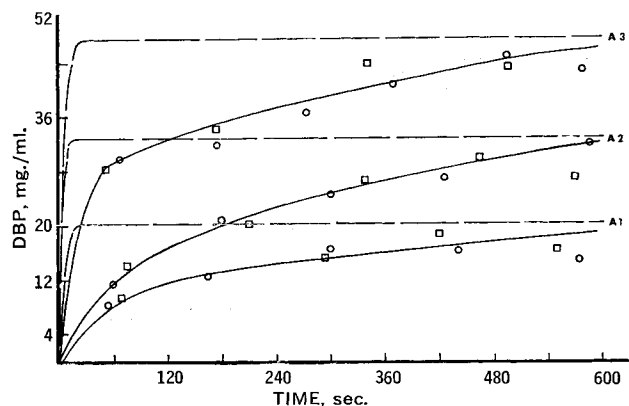


**Figure 17**—Comparison of the diffusion model theoretical curves with experimental data as functions of time, dibutyl phthalate, and surfactant concentration. Key: points, experimental data; dashed line, theoretical rate based on diffusion theory; solid line, visual fit of the data.

similar to the equation previously used to calculate  $C_{d0}$  as a function of time for the simple diffusion case (Eq. 25). The difference is the interfacial barrier constant,  $\Gamma$ , in the exponential term. Unlike the case of simple diffusion, where all the parameters could be independently determined, this  $\Gamma$  is undefined and leaves the authors incapable of independently determining its value. The magnitude

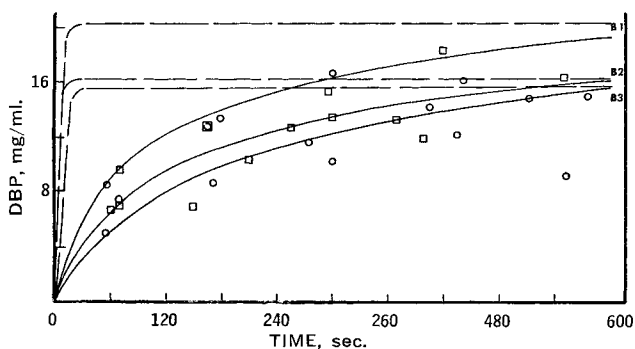


**Figure 18**—Comparison of the diffusion model theoretical curves with experimental data as functions of time and surfactant concentration for dibutyl phthalate. Key: points, experimental data; dashed line, theoretical rate based on diffusion theory; solid line, visual fit of the data.

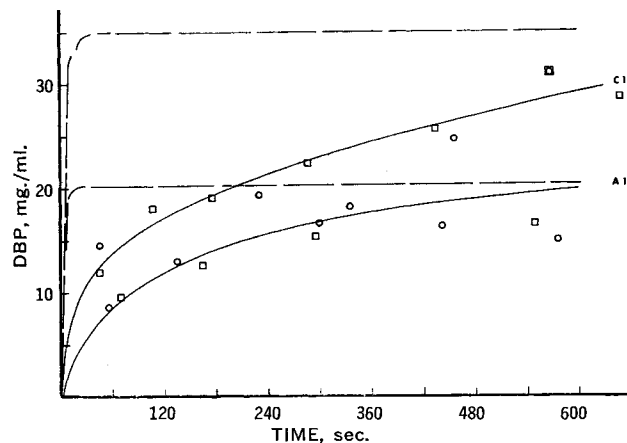


**Figure 19**—Comparison of the diffusion model theoretical curves with experimental data as functions of time and oil concentrations at 0.5% surfactant concentration for dibutyl phthalate. Key: points, experimental data; dashed line, theoretical rate based on diffusion theory; solid line, visual fit of the data.

of  $\Gamma$  can, however, be determined from the data obtained from rate experiments by suitable substitution into Eq. 24.

The rate data for the indoxole-isopropyl myristate system are shown in Fig. 15. The points are experimental and the dashed lines the theoretical values of  $C_{d0}$  calculated for simple diffusion using Eq. 25. The solid lines are theoretical, based on Eq. 24 which used values of  $\Gamma = 1.27 \times 10^{-4}$  for the 2% polysorbate 80, and  $\Gamma = 1.85 \times 10^{-4}$  for the 1% polysorbate 80. These values for  $\Gamma$  were calculated using the experimental  $C_{d0}$  values, their respective times, and Eq. 24. There is little more to be said about this interfacial barrier due to the lack of additional data for this system. However, the magnitude of the barrier is impressive, creating rates of transport about 6000 times slower than predicted by simple diffusion.

Similar treatment is afforded the dibutyl phthalate-mineral oil system. In this system, however, the interfacial barrier constant that is derived from a single rate experiment is then reapplied under varying conditions. Table V lists the surfactant concentrations, the dibutyl phthalate concentrations, and the amounts of oil used in each case. The results of the rate experiments are shown in Figs. 22–24 each at a constant surfactant concentration, with the phase volumes of oil and drug concentrations varying.

A single  $\Gamma$  was calculated from the rate data and Eq. 24 for each concentration. This  $\Gamma$  was then used in Eq. 24 to calculate theoretical  $C_{d0}$  values for all the other rate trials performed at that surfactant concentration. These results are also shown in Figs. 22, 23, and 24. The solid line represents the theoretical  $C_{d0}$  values, the points represent the experimental data, and the dashed line the theoretical

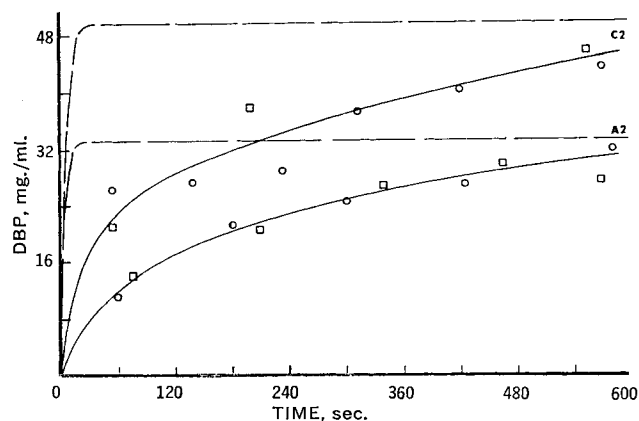


**Figure 20**—Comparison of the diffusion model theoretical curves with experimental data as functions of time and oil concentrations at 1.0% surfactant concentration for dibutyl phthalate. Key: points, experimental data; dashed line, theoretical rate based on diffusion theory; solid line, visual fit of the data.

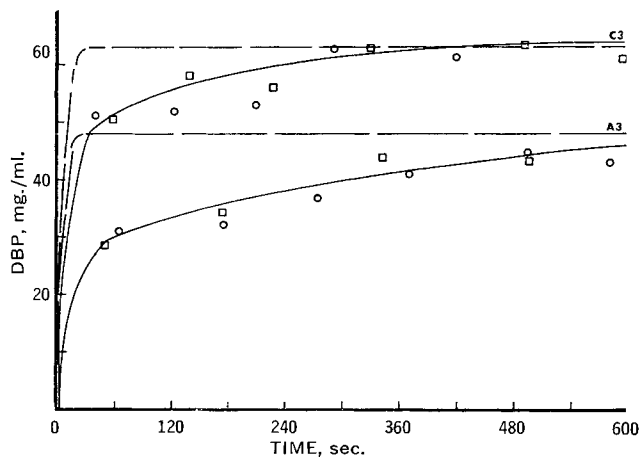


**Figure 21**—Comparison of the diffusion model theoretical curves with experimental data as functions of time and oil concentrations at 2.0% surfactant concentration for dibutyl phthalate. Key: points, experimental data; dashed line, theoretical rate based on diffusion theory; solid line, visual fit of the data.

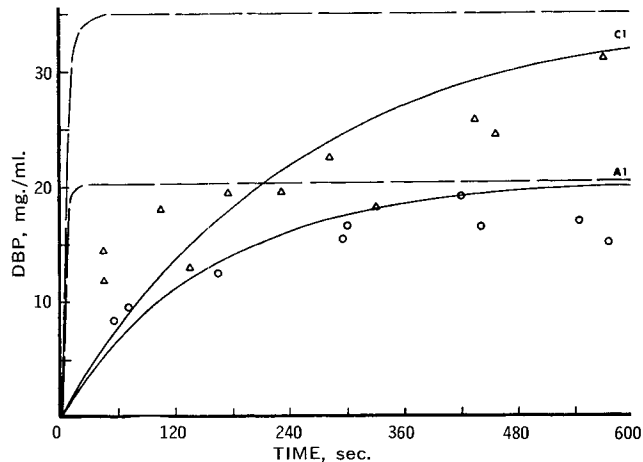


**Figure 22**—Comparison between the theoretical curves for the diffusion model, the interfacial barrier model, and the experimental data at 0.5% surfactant concentration. Key: points, experimental data; dashed line, theoretical rate based on diffusion theory; solid line, theoretical rate based on interfacial barrier theory.

values of  $C_{d0}$  based upon simple diffusion (Eq. 25). In the graph of the rates at 0.5% surfactant (Fig. 22),  $\Gamma$  was calculated to be  $2.84 \times 10^{-2}$  from Case A1, then reapplied to A1 and C1. Figure 23 depicts the rates achieved from a 1% polysorbate 80 concentration. The  $\Gamma$  value was  $2.13 \times 10^{-2}$ , calculated from Case B2. This value was then reapplied to Cases A2, B2, and C2. Figure 24 represents those rates performed at a surfactant concentration of 2%. The value of  $\Gamma$  was calculated to be  $4.53 \times 10^{-2}$  from Case B3. This value was then reapplied to Cases A3, B3, and C3.

The  $\Gamma$  values were also calculated for each experimental rate experiment performed, and are listed in Table V. The variation in  $\Gamma$  at a particular surfactant concentration is large enough to prevent distinct separation of the values from one surfactant level to the other, but it looks as if  $\Gamma$  increases with increasing surfactant concentration. Despite the deviations in the  $\Gamma$  values, when the experimental data are compared to the theoretical curves of both the simple diffusion model and the interfacial barrier model (Figs. 22, 23, and 24) there is little doubt as to its better agreement with the interfacial barrier model.

It is important that the deviations found should not be attributed solely to the barrier. The term  $A$  in the exponential portion of Eq. 24 is almost certain to add to the uncertainty of the curve-fitted constant. The definition of  $A$  is  $n4\pi a$ , which is valid only for the case of a truly mono-dispersed system. All of the emulsions used exhibited a particle size distribution which was not taken into consideration.

The discovery of an interfacial barrier in the dibutyl phthalate-mineral oil system was surprising in view of the initial experimentation involving a low viscosity medium *versus* a high viscosity medium. If, however, the required parameters, including the interfacial barrier constant, are used in Eq. 24 to calculate  $C_{d0}$  values for the case without sucrose, it was shown that at 60 sec.,  $C_{d0}$  is already at equilibrium, both theoretically and experimentally. The effect of removing the sucrose from the aqueous phase increases the

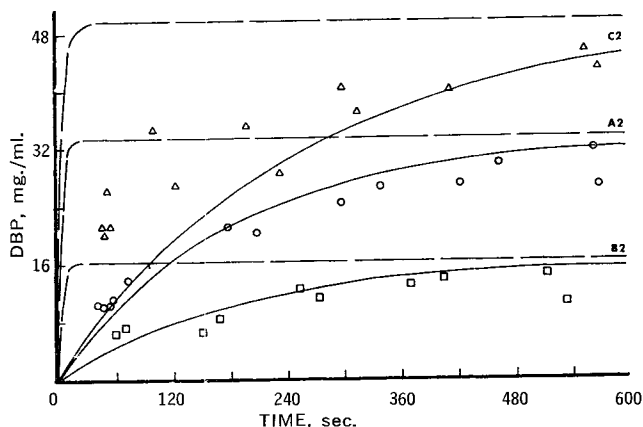


**Figure 23**—Comparison between the theoretical curves for the diffusion model, the interfacial barrier model, and the experimental data at 1.0% surfactant concentration. Key: points, experimental data; dashed line, theoretical rate based on diffusion theory; solid line, theoretical rate based on interfacial barrier theory.

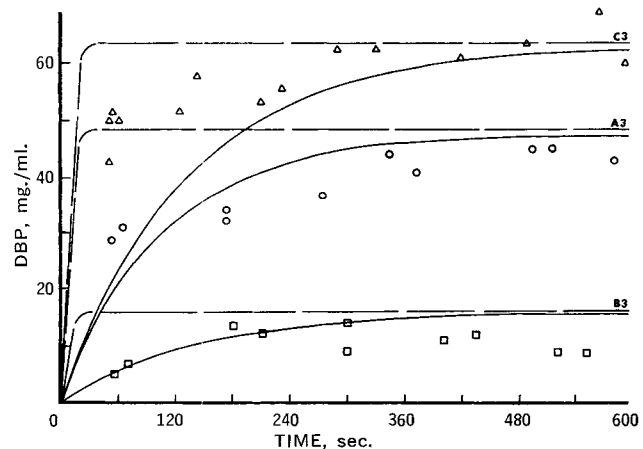


**Figure 24**—Comparison between the theoretical curves for the diffusion model, the interfacial barrier model, and the experimental data at 2.0% surfactant concentration. Key: points, experimental data; dashed line, theoretical rate based on diffusion theory; solid line, theoretical rate based on interfacial barrier theory.

**Table V**—Description of Case Notations Used in Rate Experiments

Case No.	Polysorbate 80, %	Relative Conc.	Actual Conc., mg./ml.	Oil Used, %	$\Gamma$
A 1	0.5 (0.475)	1	0.551	2	0.0284
2	1.0 (0.945)	2	1.129	2	0.0196
3	2.0 (1.880)	4	2.260	2	0.0405
B 1	0.5 (0.475)	1	0.551	2	0.0284
2	1.0 (0.945)	1	0.551	2	0.0213
3	2.0 (1.880)	1	0.585	1	0.0453
C 1	0.5 (0.475)	1	0.585	1	0.0334
2	1.0 (0.945)	2	1.165	1	0.0336
3	2.0 (1.880)	4	2.335	1	0.1218

**Table VI—Electrical Barrier Effects**

$\frac{1}{\text{Kappa}}^a$	$r^b$ ( $\times 10^6$ )	$\psi_0$ , mv.	A.U.C. <sup>c</sup> ( $\times 10^{-6}$ )	Rate, <sup>d</sup> %
6	25	25	13.60	85.8
6	50	50	66.41	17.6
6	100	100	150.58	9.8
7	25	25	11.78	98.9
7	50	50	12.16	95.8
7	100	100	24.37	47.8

<sup>a</sup> The exponential of the reciprocal of Kappa. <sup>b</sup> Assumed radii of the micelles (cm.). <sup>c</sup> Area under the curve derived by graphing the equation. <sup>d</sup> In comparison to the case where  $V^0 = 0$  is  $11.65 \times 10^6$ .

diffusion coefficients by a factor of 20. The increase in the diffusion coefficients should not account for this difference in rates, since the interfacial barrier should be rate controlling. The fact that the rates are too rapid for measurement indicates that in the absence of sucrose either the barrier is small or there is no barrier at all.

Before attributing the reduction in rates of transport solely to an interfacial barrier, the possible effects of an electrical barrier should be examined.

**CASE C—Electrical Barrier**—Various parameters involved in the potential function were evaluated numerically to determine their effects on  $V^0$  (see Eqs. 34 and 42 of Reference 1). The effects of these calculated potential functions upon the rate were then graphically evaluated for use in Eq. 41 of Reference 1. Table VI lists both, the parameters varied to obtain the various magnitudes of  $V^0$ , and the expected effects upon rates of transport.

When zeta-potentials were determined for the oil droplets in the viscous media, no electrophoretic mobility was observed. However, if the emulsion is diluted several hundred fold in water, the electrophoretic mobility pattern indicates a zeta-potential of  $-40$  mv. Neither of these measurements truly represents the surface charge, but possibly they serve to indicate the magnitude of the effect of surface charge. Examination of these results in relation to the theoretical effects listed in Table VI indicates that the slow rates of transport found could not be predicted from the effects of an electrical barrier.

### SUMMARY AND CONCLUSIONS

This study was devised to evaluate the effects of diffusion upon the rates of transport of a drug, solubilized by a surfactant, from an aqueous to a lipid phase. The experimental design was novel in that the system involved an oil phase consisting of micron sized spheres which produced an infinite diffusion layer. The basic theoretical equations proposed for the diffusion model were later modified to describe two other models—the interfacial barrier and the electrical barrier. Independent experiments were performed to determine the parameters involved in the transport process. The con-

centrations of the drug in the oil were then predicted from the appropriate equations using these independently determined parameters. Comparison of these values was made with the experimental data derived from rate experiments.

Two systems were evaluated in this manner. System I was comprised of isopropyl myristate as the lipid phase, indoxole as the drug, and polysorbate 80 as the surfactant which served to solubilize the drug and also form the emulsion. System II was formed with mineral oil as the lipid phase, dibutyl phthalate as the drug, and polysorbate 80 in 75% sucrose solution as the aqueous phase to facilitate the measurement of rates of transport.

Theoretically, if diffusion through the aqueous phase was the rate determining step in the transport process, then the transport of the drug should have occurred at rates too fast for measurement. However, the rates of transport were slow enough for measurement in both systems. In System I, the rates of transport were 6000 times slower than would have been predicted from diffusion theory, while System II produced rates about 25 times slower.

The equation for the interfacial barrier was then used to determine the magnitude of the barrier necessary to produce the observed rates. A comparison of the barrier expected from electrical effects and the experimental data indicated that the electrical barrier could not be large enough to produce the low rates of transport experimentally determined. The theoretical model for an interfacial barrier provided the best agreement with the experimental data derived from the rate experiments and therefore is proposed as the rate determining mechanism in the transport process.

### REFERENCES

- (1) A. H. Goldberg, W. I. Higuchi, N. F. H. Ho, and G. Zografi, *J. Pharm. Sci.*, **56**, 1432(1967).
- (2) A. H. Ghanem, W. I. Higuchi, and A. P. Simonelli, *ibid.*, **58**, 165(1969).
- (3) T. R. Bates, M. Gibaldi, and J. L. Kanig, *ibid.*, **55**, 191(1966).
- (4) A. H. Goldberg and W. I. Higuchi, *ibid.*, **57**, 1583(1968).
- (5) A. H. Goldberg, G. Zografi, and W. I. Higuchi, *ibid.*, **56**, 309(1967).

### ACKNOWLEDGMENTS AND ADDRESSES

Received June 4, 1969 from the *College of Pharmacy, University of Michigan, Ann Arbor, MI 48104*

Accepted for publication July 31, 1969.

Supported in part by grant GM-13368-01 and fellowship A-F1-GM-34,237-01 from the National Institutes of Health, U.S.P.H.S., Bethesda, Md.

\* Present address: Department of Pharmaceutics, College of Pharmaceutical Sciences, Columbia University, 115 West 68th St., New York, NY 10023